Electronic Supplementary Material (ESI) for Dalton Transactions.
This journal is © The Royal Society of Chemistry 2021

Supporting Information

Structural, magnetic and theoretical analyses of anionic and cationic phthalocyaninato-terbium(III) double-decker complexes: Magnetic relaxation via higher ligand-field sublevels enhanced by oxidation

Yoji Horii,[a]* Marko Damjanović,* Keiichi Katoh [b]* and Masahiro Yamashita [c,d]*

[a.] *Department of Chemistry, Faculty of Science, Nara Women's University, Nara 630-8506, Japan*

[b.] *Department of Chemistry, Graduate School of Science, Josai University, 1-1 Keyakidai, Sakado, Saitama 350-0295, Japan*

[c.] *Department of Chemistry, Graduate School of Science, Tohoku University, 6-3 Aza-Aoba Aramaki, Aoba-ku, Sendai, Miyagi 980-8578, Japan*

[d.] *School of Materials Science and Technology, Nankai University, Tianjin 300350, China*

Physical properties measurements

Single-crystal X-ray diffraction measurements were performed using a Rigaku Varimax with Saturn724+ with CrysAlisPro 1.171.40.53[1] and a Rigaku VariMax with RAPID II with RAPID AUTO. Initial structures were obtained using SHELXT (2018/3) and refined with SHELXL (2018/3)[2] combined with Yadokari-XG.[3] For the analyses of the crystal structures of $\mathbf{1}^{-}$ at 263 K, SQUEEZE[4] command of platon was used to consider the disordered DMSO molecule. Powder X-ray diffraction (PXRD) pattern was acquired by Rigaku RINT-2000 using glass capillary and Bruker D2 PHASER. Simulated PXRD patterns were obtained from the cif file using Mercury 4.1.0.[5] Magnetic measurements were performed on Quantum Design SQUID magnetometers MPMS-XL, MPMS3, and the ACMS option of PPMS MODEL 6000.

Preparation of magnetically diluted samples

Magnetically diluted samples of $\mathbf{1}^{-}$ and $\mathbf{1}^{+}$, denoted as $\mathbf{1}^{-*}$ and $\mathbf{1}^{+*}$, respectively, were prepared by doping **1** to an excess amount of Y^{3+} analogue (**1Y**). **1Y** was prepared according to the literature method.[6]

Preparation of $\mathbf{1}^{-*}$

7.08 mg of **1** (0.0030 mmol) and 60.80 mg (0.027 mmol) of **1Y** were dissolved in 2 mL of dichloromethane, and the solution was stirred overnight. After evaporation of the solvent, 10 mL of dimethyl sulfoxide and 500 mL of hydrazine monohydrate were added, and the mixture was ultrasonicated until the solid mixture was completely dissolved in DMSO (ca. 30 min). Addition of 107 mg of TBA·Br to the light blue reaction solution afforded purple precipitation. The reaction mixture was filtrated, and the purple solid was washed with 10 mL of DMSO (67.1 mg, 87%).

Preparation of $\mathbf{1}^{+*}$

9.37 mg of **1** (0.0040 mmol) and 78.79 mg of **1Y** (0.035 mmol) were dissolved in ~10 mL of toluene, and the solution was stirred overnight. 30 mg of $SbCl_6$·Ox (0.056 mmol) were added, and the mixture was ultrasonicated for 5 min. The vial was placed in the oven and heated at 100 °C for 5 h, followed by slow cooling down to room temperature over 12 h to afford the crystalline $\mathbf{1}^{+*}$ (88.1 mg, 87%).

Debye model equations

Magnetic relaxation time τ was obtained by simultaneously fitting the real (χ_M') and imaginary (χ_M'') parts of the ac magnetic susceptibilities using the following generalized Debye model equations:

$$\chi_M' = \chi_S + (\chi_T - \chi_S)\frac{(2\pi\tau)^{1-\alpha}\sin\left(\frac{\pi\alpha}{2}\right)}{1 + 2(2\pi\tau)^{1-\alpha}\sin\left(\frac{\pi\alpha}{2}\right) + (2\pi\tau)^{2-2\alpha}} \quad \text{eq. S1a}$$

$$\chi_M'' = (\chi_T - \chi_S)\frac{(2\pi\tau)^{1-\alpha}\cos\left(\frac{\pi\alpha}{2}\right)}{1 + 2(2\pi\tau)^{1-\alpha}\sin\left(\frac{\pi\alpha}{2}\right) + (2\pi\tau)^{2-2\alpha}} \quad \text{eq. S1b}$$

where χ_T is the isothermal magnetic susceptibility, χ_S is the adiabatic magnetic susceptibility and α is the dispersion factor. Optimized parameters are summarized in Tables S3-S6.

Table S1. Crystallographic data for 1$^-$ and 1$^+$.

	1$^-$		**1$^+$**
T / K	120	263	120
Crystal system	Monoclinic	Monoclinic	Triclinic
Space group	$P2_1/c$	$P2_1/c$	P-1
Formula	$C_{146}H_{200}N_{17}O_{17}STb$	$C_{146}H_{200}N_{17}O_{17}STb$	$C_{191}H_{232}Cl_6N_{16}O_{16}SbTb$
Z	4	4	2
a / Å	20.1606(4)	20.6206(4)	16.3767(2)
b / Å	30.2161(6)	30.5969(5)	24.6005(3)
c / Å	23.2154(16)	23.4609(5)	24.8548(2)
α / °	90	90	65.8000(10)
β / °	102.336(7)	101.534(2)	78.6380(10)
γ / °	90	90	80.6740(10)
V / Å^3	13815.7(11)	14503.2(5)	8917.33(19)
ρ / g cm^{-3}	1.277	1.182	1.304
R_1	0.0816	0.0608	0.0531
wR_2	0.2020	0.1487	0.1357
GOF	1.070	1.034	1.007
CCDC number	1973905	2085462	1973906

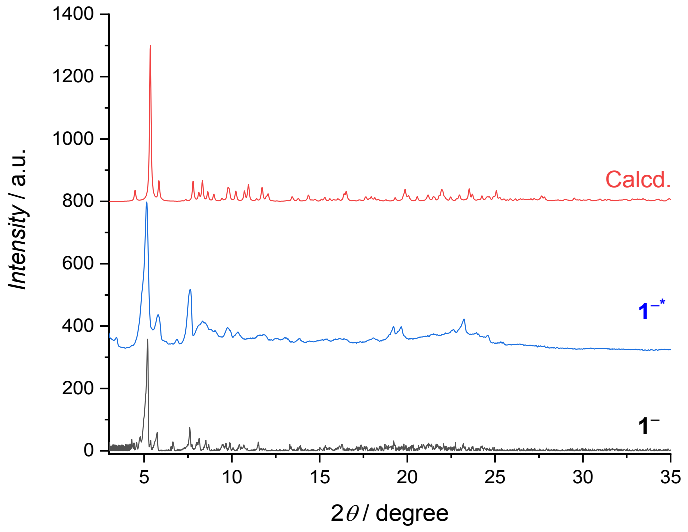

Figure S1. Experimental (lower) and calculated (upper) power X-ray diffraction patterns for $\mathbf{1}^{-}$ and $\mathbf{1}^{-*}$.

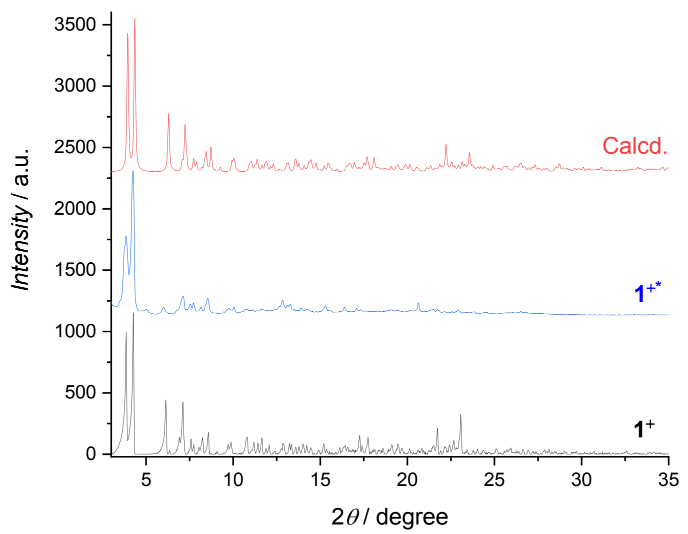

Figure S2. Experimental (lower) and calculated (upper) power X-ray diffraction patterns for $\mathbf{1}^{+}$ and $\mathbf{1}^{+*}$.

Frequency calculation

Geometry optimization and analytical frequency calculations were performed at B3LYP/Def2-SVP[7-8] level of theory using the software ORCA 4.2.1[9]. A RIJCOSX approximation using Def2/J[10] auxiliary basis was applied to reduce the computational costs. Initial structures for calculations were made based on the crystal structures. To reduce the computational costs, the Tb atom and *n*-butoxy chains were replaced by an Y atom and methoxy groups. After the calculation, the atomic weight of Y was changed to that of Tb using orca_vib module to get better agreement between the experimental and the theoretical IR spectra. Frequency calculation using the cif of **1**$^{-}$ (indicated as **1***$^{-}$ in Table S2) afforded one imaginary frequency, while the calculations using the crystal structure of **1**$^{+}$ (indicated as **1**$^{-}$) showed no imaginary frequency.

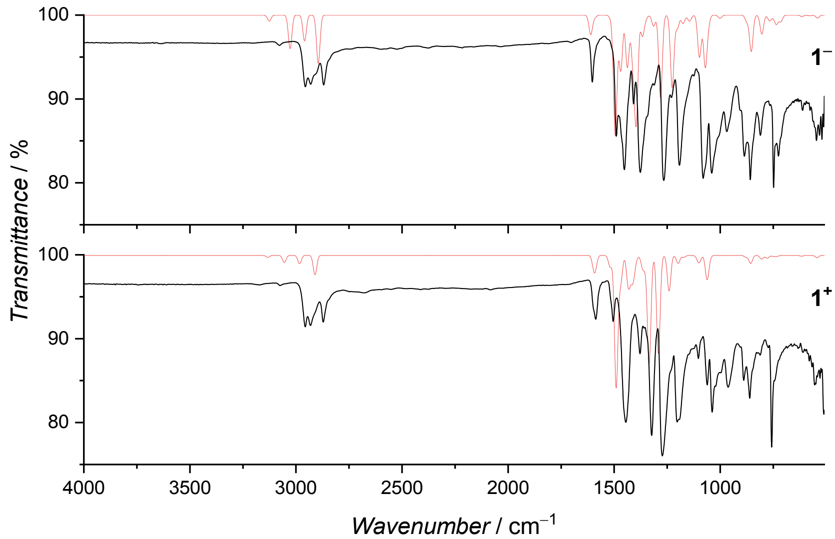

Figure S3. Experimental (black lines) and calculated (red lines) IR spectra for **1**$^{-}$ and **1**$^{+}$. A Gaussian type lineshape function with 20 cm^{-1} of FWHM and a vibrational frequency scaling factor (0.97) were applied for calculated vibrational mode and transition moment.

Table S2. Calculated molecular vibrational frequencies for 1*⁻, 1⁻ and 1⁺.

No.	*Wavenumber* / cm^{-1}		
	1*$^{-}$	**1**$^{-}$	**1**$^{+}$
1	-7.51	6.99	9.68
2	8.56	10.37	10.35
3	10.46	10.80	12.82
4	11.13	12.40	12.96
5	12.47	12.54	13.58
6	13.79	15.25	16.39
7	21.97	21.73	23.06
8	24.20	24.92	25.43
9	24.71	25.52	26.01
10	30.21	30.60	31.26
11	31.91	31.10	31.91
12	36.22	35.76	35.43
13	37.57	35.90	35.48
14	39.75	39.04	38.93
15	40.35	40.18	40.62
16	41.73	40.41	41.73
17	42.37	40.52	42.00
18	50.00	49.92	50.69
19	50.39	50.05	50.71
20	54.41	54.90	56.21
21	55.45	54.95	56.28
22	63.64	66.24	67.57
23	68.25	66.72	68.10
24	72.02	74.16	78.10
25	74.10	74.52	78.51
26	74.78	75.13	79.28
27	74.99	75.62	79.77
28	75.58	76.62	82.86
29	76.73	76.80	83.08
30	78.79	78.02	83.31
31	82.36	82.65	88.29
32	92.10	95.17	100.74
33	92.49	95.46	100.94
34	95.98	102.48	103.47
35	98.86	103.08	103.64
36	103.00	103.22	107.05
37	103.72	103.43	107.34
38	106.14	108.01	111.72
39	108.16	108.26	112.02
40	109.22	112.60	113.54
41	113.07	119.57	118.77
42	114.59	121.38	120.85
43	120.68	123.59	123.15
44	124.92	123.93	123.42
45	125.86	129.79	131.62
46	130.06	129.82	136.52
47	130.51	130.45	136.57
48	131.02	130.47	136.74
49	131.87	131.90	136.80
50	132.47	131.99	139.34
51	135.07	134.76	139.77
52	147.94	154.54	154.50
53	153.24	154.68	155.02
54	154.40	155.00	157.63
55	155.61	155.46	157.75
56	156.63	162.30	164.75
57	161.75	162.52	165.27
58	165.68	170.31	169.40
59	166.95	170.71	169.61
60	168.86	171.04	170.47
61	169.33	171.40	170.60
62	171.09	181.83	177.07
63	172.37	182.00	177.12
64	181.64	185.98	183.98
65	184.43	186.06	184.22
66	185.91	196.62	191.12
67	186.36	196.75	191.30
68	196.85	198.01	196.18
69	197.02	198.07	196.39
70	197.48	204.07	196.61
71	202.47	204.82	197.15
72	203.54	208.48	204.42
73	204.51	211.59	206.97
74	206.08	212.82	207.56
75	211.00	213.19	210.32
76	212.43	214.18	210.66
77	214.41	214.26	210.85
78	216.08	215.84	213.24
79	216.82	215.95	213.61
80	217.86	222.35	219.42
81	221.61	222.76	219.74
82	223.84	224.97	223.30
83	224.60	228.61	226.54
84	226.78	234.19	226.97
85	235.06	234.82	227.40
86	238.03	241.03	236.72
87	242.50	241.54	236.83
88	249.57	251.00	242.58
89	250.99	251.26	242.81
90	258.14	264.46	251.73
91	261.10	264.50	252.01
92	263.85	265.15	252.93
93	264.36	265.38	253.33
94	264.72	269.38	257.71
95	265.03	271.74	261.60
96	270.07	275.64	262.11
97	272.69	276.50	262.70
98	275.58	277.32	267.05
99	276.12	278.18	267.67
100	276.51	278.42	270.41
101	278.14	278.77	271.72
102	278.72	280.40	272.00
103	279.62	280.60	272.31
104	280.24	287.25	276.63
105	287.35	287.39	277.32
106	288.08	287.71	285.43
107	288.91	287.93	285.63
108	297.39	289.40	285.67
109	302.37	289.89	285.85
110	324.51	325.40	312.71
111	325.19	325.48	312.85
112	328.68	342.16	326.47
113	332.00	342.22	326.59
114	341.72	343.33	328.22
115	342.44	343.76	328.96
116	343.61	362.29	348.51
117	349.37	366.52	352.28
118	362.44	377.42	375.20
119	367.04	377.59	375.51
120	377.57	388.95	386.34
121	384.36	390.14	386.61
122	389.22	390.25	386.75
123	390.12	390.46	387.02
124	390.27	390.53	387.37
125	390.62	390.68	388.80
126	406.06	405.87	392.55
127	406.98	406.29	393.15
128	407.80	407.12	397.74
129	408.54	407.28	397.77
130	411.26	408.33	399.52
131	422.64	408.49	399.70
132	425.03	424.81	412.68
133	430.61	425.33	413.07
134	449.12	471.68	464.99
135	454.37	472.12	465.19
136	470.50	472.44	477.94
137	472.88	472.57	478.01
138	473.09	472.74	478.40
139	473.15	472.85	478.47
140	473.36	472.96	478.71
141	473.45	473.07	478.73
142	474.75	473.73	479.17
143	481.16	474.09	479.47
144	484.79	484.91	481.65
145	485.44	484.97	481.79
146	485.70	485.70	482.50
147	486.81	485.77	482.58
148	491.27	491.44	484.65
149	497.26	491.56	485.56
150	497.40	497.35	493.36
151	497.50	497.40	493.41
152	504.03	497.46	493.91
153	507.46	497.56	493.97
154	510.20	510.05	511.31
155	526.19	510.20	511.45
156	528.68	528.32	530.20
157	530.27	530.20	530.32
158	533.30	530.31	542.62
159	537.12	533.53	547.27
160	543.85	545.12	550.04
161	547.41	548.19	552.18
162	549.59	556.67	558.58
163	557.36	557.86	558.72
164	558.01	557.95	560.40
165	558.15	558.02	560.63
166	559.92	558.24	560.68
167	569.84	558.32	560.77
168	594.03	594.09	599.44
169	596.01	594.50	599.67
170	598.36	597.91	601.95
171	601.56	598.43	602.46
172	627.83	632.74	634.99
173	632.89	632.80	635.07
174	633.11	633.28	635.62
175	633.61	633.32	635.72
176	635.65	646.41	646.74
177	646.50	646.44	646.78
178	656.51	656.75	655.34
179	658.66	656.93	655.47
180	680.20	680.86	682.77
181	682.44	682.76	684.44
182	700.63	700.98	696.60
183	701.37	701.69	697.29
184	722.62	722.24	725.98
185	722.73	722.42	726.93
186	722.79	722.59	728.30
187	723.15	722.62	728.42
188	725.43	722.73	728.83
189	725.64	722.99	728.98
190	726.56	725.23	729.14
191	727.10	725.48	729.92
192	729.76	729.37	732.88
193	730.09	729.56	733.03
194	734.33	734.27	733.74
195	734.64	734.64	733.83
196	736.05	734.80	733.99
197	736.61	734.91	734.21
198	743.56	736.80	734.60
199	746.07	736.88	734.76
200	754.77	754.77	756.59
201	755.35	754.84	756.77
202	756.38	757.88	756.90
203	757.69	758.15	756.96
204	758.44	758.28	758.55
205	758.74	758.42	758.63
206	760.37	760.09	763.71
207	760.48	760.14	763.92
208	761.72	761.21	768.87
209	763.74	761.39	769.10
210	769.72	771.65	774.45
211	772.34	772.87	775.20
212	774.71	775.79	777.53
213	775.94	775.97	777.75
214	790.35	790.63	787.83
215	791.96	792.15	793.86
216	793.66	793.55	797.99
217	794.82	793.62	799.52
218	797.42	797.51	799.79
219	797.80	797.71	800.34
220	797.89	797.75	800.48

221	798.23	797.89	801.34	298	1172.87	1172.83	1169.20	375	1453.56	1454.28	1451.68
222	798.66	798.05	801.54	299	1172.87	1172.86	1169.22	376	1454.55	1454.85	1452.63
223	799.41	798.15	802.28	300	1173.08	1172.94	1169.23	377	1455.05	1454.89	1452.75
224	822.37	828.66	829.86	301	1174.34	1172.98	1169.29	378	1455.60	1461.36	1456.46
225	828.96	828.74	829.97	302	1174.96	1178.66	1169.34	379	1455.76	1461.38	1456.63
226	829.00	829.13	830.88	303	1179.27	1178.78	1169.39	380	1460.83	1461.44	1460.28
227	829.88	829.16	830.96	304	1179.64	1180.46	1169.40	381	1461.25	1461.49	1466.28
228	856.55	866.27	868.01	305	1183.43	1180.66	1169.45	382	1461.39	1461.52	1466.41
229	866.53	866.60	868.37	306	1194.32	1195.93	1169.57	383	1461.54	1461.56	1466.51
230	870.40	876.92	878.31	307	1195.93	1196.07	1169.59	384	1461.57	1461.63	1466.57
231	876.30	877.04	878.50	308	1198.87	1203.45	1175.46	385	1461.61	1461.65	1466.62
232	876.89	878.98	881.78	309	1201.62	1204.60	1175.82	386	1461.67	1462.09	1466.67
233	877.64	879.01	882.66	310	1203.61	1205.42	1202.64	387	1461.95	1462.18	1466.74
234	879.17	879.87	882.86	311	1204.23	1205.49	1202.86	388	1462.06	1462.20	1466.78
235	879.42	879.90	883.18	312	1205.13	1205.65	1202.94	389	1462.07	1462.28	1467.15
236	880.07	880.01	883.29	313	1205.47	1205.72	1202.99	390	1462.15	1462.30	1467.25
237	885.08	886.54	887.61	314	1205.66	1206.37	1203.10	391	1462.34	1462.37	1467.32
238	890.77	891.07	892.14	315	1206.58	1206.72	1203.21	392	1462.42	1462.48	1467.43
239	891.45	891.30	892.37	316	1207.93	1209.03	1204.83	393	1462.52	1462.49	1467.45
240	892.32	891.58	892.59	317	1208.74	1209.26	1205.06	394	1465.19	1467.47	1467.55
241	892.49	892.02	892.77	318	1209.17	1211.66	1207.51	395	1467.42	1467.57	1467.64
242	893.02	892.33	893.00	319	1209.46	1211.71	1207.62	396	1467.84	1467.71	1467.67
243	893.15	892.69	893.37	320	1211.74	1211.89	1207.69	397	1469.46	1469.96	1472.76
244	895.11	892.93	893.58	321	1211.88	1212.02	1207.98	398	1475.99	1476.16	1472.98
245	896.41	892.98	893.72	322	1215.76	1219.83	1208.04	399	1476.49	1476.76	1473.45
246	900.56	900.64	905.21	323	1219.94	1220.79	1208.17	400	1477.31	1479.96	1474.55
247	900.76	900.74	905.29	324	1224.03	1237.14	1212.13	401	1480.13	1479.99	1474.56
248	901.98	900.87	905.53	325	1226.66	1237.19	1212.39	402	1480.46	1480.55	1474.78
249	902.06	901.16	905.66	326	1237.06	1239.01	1235.49	403	1480.85	1480.62	1474.96
250	902.83	901.56	905.95	327	1238.81	1239.12	1235.57	404	1480.93	1480.85	1475.07
251	903.14	902.28	906.57	328	1239.06	1239.29	1235.71	405	1481.09	1480.91	1475.58
252	935.35	902.47	906.79	329	1239.44	1239.36	1235.76	406	1481.65	1481.01	1475.63
253	935.56	903.36	907.85	330	1240.96	1242.43	1235.96	407	1481.91	1482.11	1475.72
254	1020.80	1024.40	1019.17	331	1242.49	1242.86	1236.06	408	1482.14	1482.20	1476.19
255	1021.52	1024.71	1019.55	332	1243.64	1246.14	1239.03	409	1482.25	1482.47	1476.59
256	1024.30	1031.92	1028.82	333	1245.93	1246.69	1239.10	410	1482.56	1482.51	1476.63
257	1030.62	1031.99	1028.85	334	1246.41	1264.28	1279.37	411	1482.68	1482.64	1476.71
258	1031.95	1032.28	1030.08	335	1250.75	1264.43	1279.56	412	1483.13	1482.70	1476.76
259	1032.03	1032.39	1030.12	336	1264.75	1264.71	1279.72	413	1483.38	1482.83	1477.33
260	1037.11	1043.80	1036.49	337	1265.21	1265.76	1280.05	414	1483.63	1482.93	1477.49
261	1043.72	1044.23	1037.90	338	1265.73	1265.91	1280.08	415	1484.26	1484.18	1477.69
262	1070.05	1088.09	1077.09	339	1266.22	1266.49	1280.83	416	1484.42	1484.22	1477.80
263	1071.66	1088.12	1077.12	340	1266.64	1266.73	1280.93	417	1484.95	1484.81	1479.93
264	1087.15	1089.09	1080.45	341	1267.53	1267.33	1282.53	418	1485.39	1485.88	1484.60
265	1088.06	1089.13	1080.57	342	1309.85	1316.03	1327.90	419	1486.39	1485.96	1484.67
266	1088.58	1090.02	1080.75	343	1313.55	1316.96	1330.83	420	1504.62	1505.98	1486.19
267	1089.50	1090.04	1080.78	344	1316.40	1317.41	1331.01	421	1506.44	1506.74	1486.33
268	1089.69	1093.18	1081.02	345	1317.40	1319.13	1331.15	422	1507.11	1513.48	1511.09
269	1092.40	1093.31	1081.09	346	1318.56	1319.88	1331.35	423	1510.62	1513.77	1511.80
270	1093.07	1093.48	1081.88	347	1320.03	1319.95	1331.81	424	1511.48	1514.26	1514.54
271	1093.44	1093.57	1081.99	348	1320.69	1321.17	1331.92	425	1513.98	1514.48	1514.66
272	1097.45	1102.81	1088.00	349	1321.42	1321.27	1333.04	426	1514.45	1514.94	1514.84
273	1102.17	1102.90	1093.45	350	1347.21	1348.46	1365.61	427	1516.42	1517.47	1515.39
274	1103.09	1103.74	1093.50	351	1349.15	1348.63	1366.50	428	1516.57	1518.07	1515.52
275	1103.96	1103.82	1094.55	352	1353.13	1353.85	1371.59	429	1518.60	1518.79	1517.38
276	1119.82	1124.18	1094.61	353	1353.74	1354.65	1371.97	430	1523.18	1526.83	1518.12
277	1125.44	1124.50	1118.09	354	1354.35	1354.73	1376.01	431	1527.32	1527.22	1521.84
278	1129.04	1131.29	1126.11	355	1355.72	1354.88	1376.22	432	1529.97	1531.60	1535.98
279	1131.09	1131.69	1132.85	356	1374.70	1391.31	1391.14	433	1531.60	1532.82	1536.29
280	1132.82	1136.56	1133.52	357	1375.90	1393.86	1397.97	434	1532.44	1538.24	1536.69
281	1136.65	1136.94	1137.81	358	1392.21	1396.63	1405.03	435	1538.59	1538.35	1536.91
282	1138.30	1137.77	1141.92	359	1396.75	1396.71	1405.46	436	1539.77	1540.70	1541.58
283	1138.73	1139.96	1141.99	360	1396.83	1397.50	1405.67	437	1540.95	1540.84	1542.06
284	1155.24	1159.83	1154.82	361	1397.17	1397.72	1405.74	438	1548.38	1549.88	1563.21
285	1159.82	1159.88	1154.86	362	1397.66	1399.76	1406.16	439	1549.76	1550.03	1563.28
286	1168.70	1172.33	1156.29	363	1400.09	1400.50	1406.38	440	1551.18	1550.97	1566.15
287	1169.38	1172.35	1156.40	364	1408.55	1409.06	1411.19	441	1551.95	1551.11	1568.25
288	1171.75	1172.42	1157.91	365	1431.63	1432.50	1411.90	442	1562.02	1563.58	1568.37
289	1172.01	1172.55	1158.12	366	1432.89	1435.82	1420.74	443	1564.22	1564.68	1571.94
290	1172.02	1172.56	1165.87	367	1435.85	1435.88	1441.09	444	1607.05	1607.35	1628.88
291	1172.30	1172.61	1165.93	368	1437.85	1438.97	1441.21	445	1608.19	1608.36	1629.95
292	1172.34	1172.62	1168.80	369	1438.74	1439.06	1441.51	446	1633.18	1640.73	1637.13
293	1172.45	1172.64	1168.92	370	1447.28	1451.53	1447.62	447	1634.40	1641.08	1638.08
294	1172.57	1172.66	1168.96	371	1451.20	1451.97	1447.70	448	1640.64	1641.49	1638.33
295	1172.67	1172.70	1169.06	372	1451.78	1452.37	1450.04	449	1640.70	1641.63	1638.63
296	1172.68	1172.74	1169.08	373	1452.06	1452.67	1450.31	450	1641.12	1641.70	1638.65
297	1172.83	1172.80	1169.14	374	1452.69	1454.17	1450.66	451	1641.49	1642.27	1638.84

452	1642.12	1642.46	1639.16	477	2992.45	2985.60	3001.32	502	3121.11	3121.27	3149.53
453	1642.92	1643.70	1639.27	478	3049.35	3049.87	3074.09	503	3121.60	3121.31	3149.61
454	1658.66	1658.63	1646.64	479	3050.18	3050.07	3074.63	504	3121.69	3121.40	3149.62
455	1659.44	1659.40	1646.77	480	3050.37	3050.12	3074.64	505	3121.75	3121.43	3149.75
456	1659.84	1659.92	1647.13	481	3050.55	3050.29	3074.79	506	3122.72	3121.73	3150.04
457	1660.17	1660.34	1647.62	482	3050.63	3050.37	3074.80	507	3122.83	3121.77	3150.06
458	1660.25	1660.70	1647.70	483	3051.00	3050.44	3074.96	508	3124.21	3121.94	3150.16
459	1661.44	1660.95	1647.91	484	3051.37	3050.53	3075.00	509	3124.64	3122.05	3150.25
460	1664.30	1661.36	1648.41	485	3051.77	3050.63	3075.13	510	3207.37	3220.14	3227.15
461	1664.72	1661.99	1649.93	486	3052.18	3050.73	3075.15	511	3208.86	3220.22	3227.34
462	2983.24	2983.04	2999.00	487	3053.08	3050.90	3075.19	512	3218.74	3220.92	3227.97
463	2983.63	2983.22	2999.34	488	3054.35	3050.97	3075.29	513	3219.63	3220.96	3228.14
464	2983.65	2983.34	2999.48	489	3058.71	3051.01	3075.42	514	3220.16	3221.18	3228.38
465	2983.69	2983.39	2999.49	490	3059.10	3051.21	3075.59	515	3220.32	3221.45	3228.50
466	2983.99	2983.62	2999.72	491	3059.96	3051.37	3075.62	516	3220.34	3221.50	3228.55
467	2984.36	2983.66	2999.75	492	3075.22	3051.47	3075.76	517	3220.57	3221.72	3228.60
468	2984.96	2983.88	2999.94	493	3075.52	3051.55	3075.84	518	3220.69	3221.78	3228.71
469	2985.17	2984.13	3000.07	494	3117.22	3120.15	3148.33	519	3221.85	3221.88	3228.88
470	2985.67	2984.39	3000.19	495	3117.60	3120.27	3148.49	520	3222.16	3222.55	3229.53
471	2986.23	2984.51	3000.42	496	3120.25	3120.34	3148.70	521	3222.24	3222.94	3229.87
472	2986.36	2984.60	3000.54	497	3120.71	3120.42	3148.75	522	3222.35	3223.14	3230.05
473	2987.74	2984.78	3000.59	498	3120.82	3120.61	3148.80	523	3222.61	3223.32	3230.14
474	2989.68	2984.92	3000.72	499	3120.87	3120.98	3149.03	524	3223.61	3223.41	3230.31
475	2990.43	2985.03	3000.85	500	3120.92	3121.03	3149.15	525	3224.24	3223.58	3230.36
476	2992.20	2985.12	3000.99	501	3120.99	3121.23	3149.23				

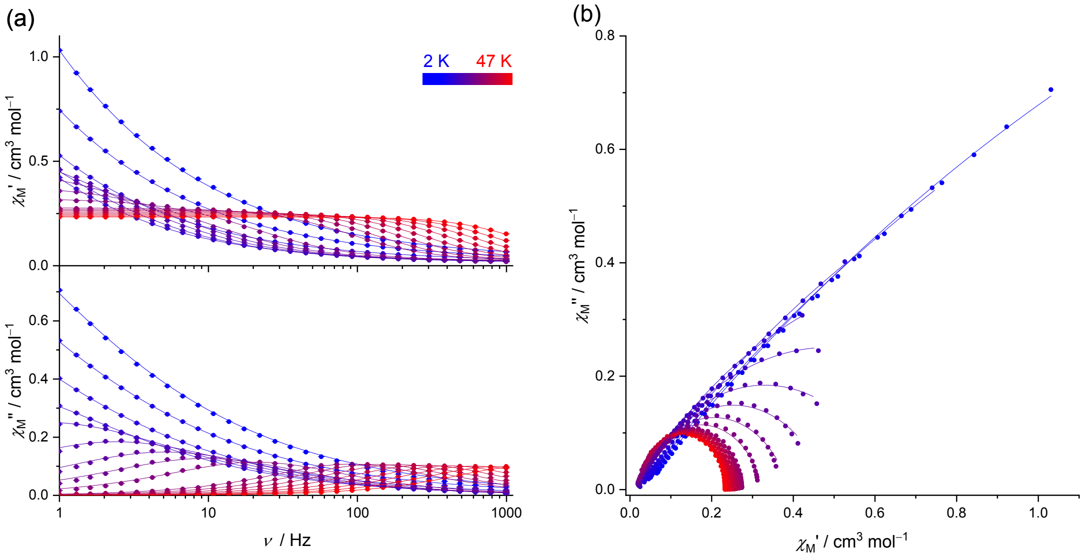

Figure S4. (a) AC magnetic susceptibilities and (b) Argand plots of **1**⁻ without a bias dc field. Solid curves represent the fit using generalized Debye model equations.

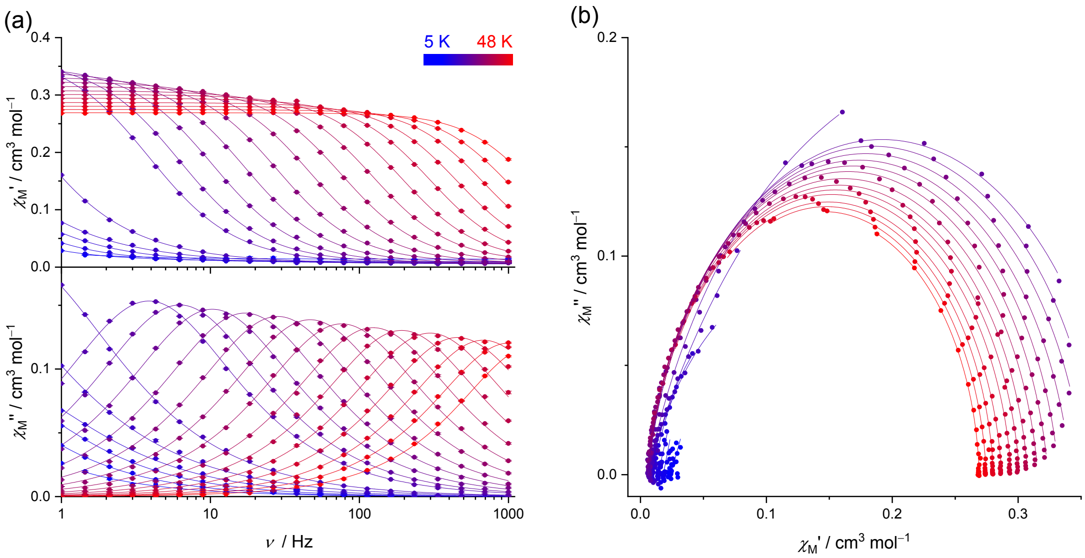

Figure S5. (a) AC magnetic susceptibilities and (b) Argand plots of **1**⁻ at 2000 Oe bias dc field. Solid curves represent the fit using generalized Debye model equations.

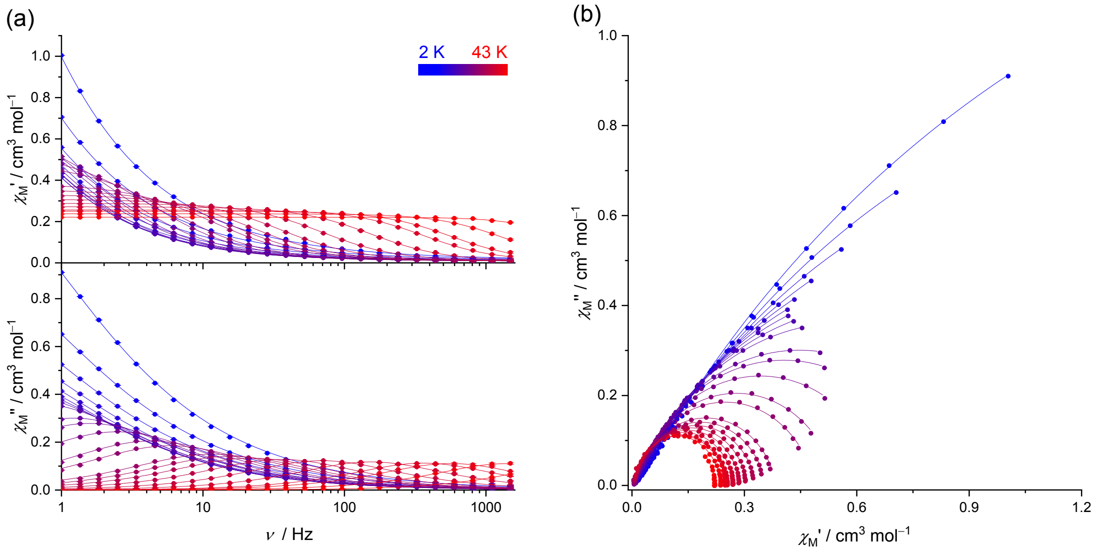

Figure S6. (a) AC magnetic susceptibilities and (b) Argand plots of $\mathbf{1}^{+}$ without a bias dc field. Solid curves represent the fit using generalized Debye model equations.

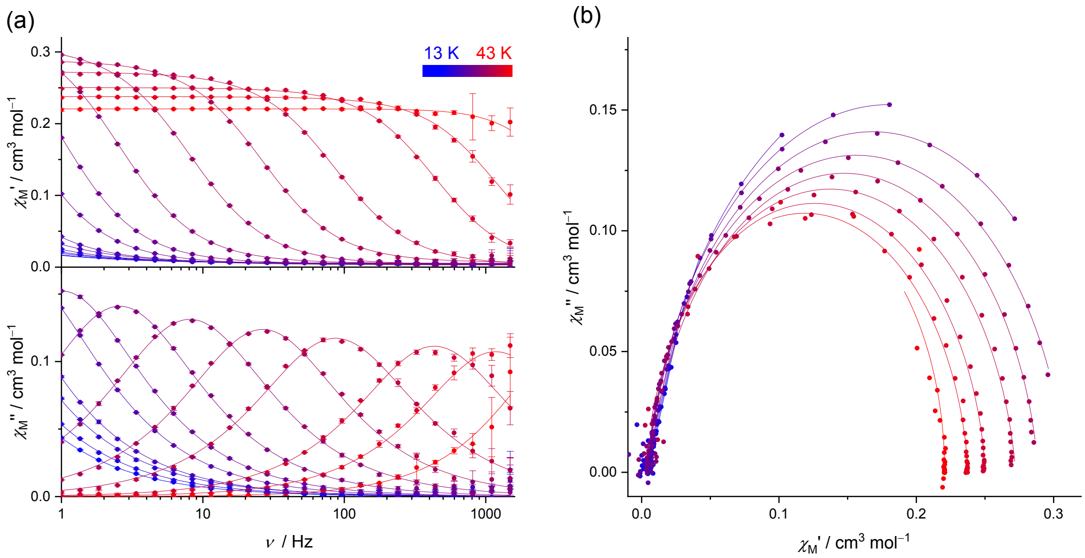

Figure S7. (a) AC magnetic susceptibilities and (b) Argand plots of $\mathbf{1}^{+}$ at 2000 Oe bias dc field. Solid curves represent the fit using generalized Debye model equation

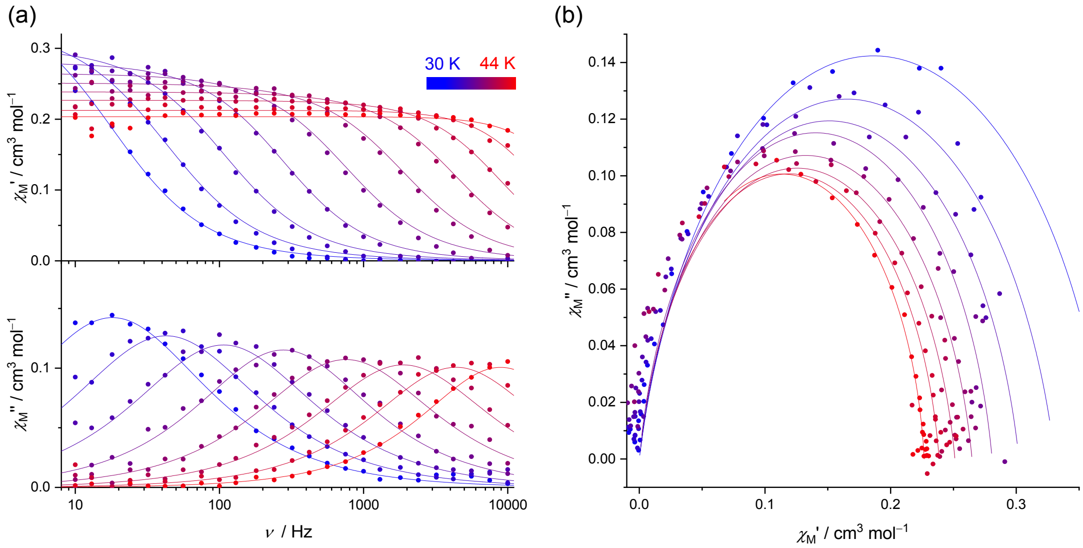

Figure S8. (a) AC magnetic susceptibilities and (b) Argand plots of $\mathbf{1}^{-*}$ without a bias dc field. Solid curves represent the fit using generalized Debye model equations.

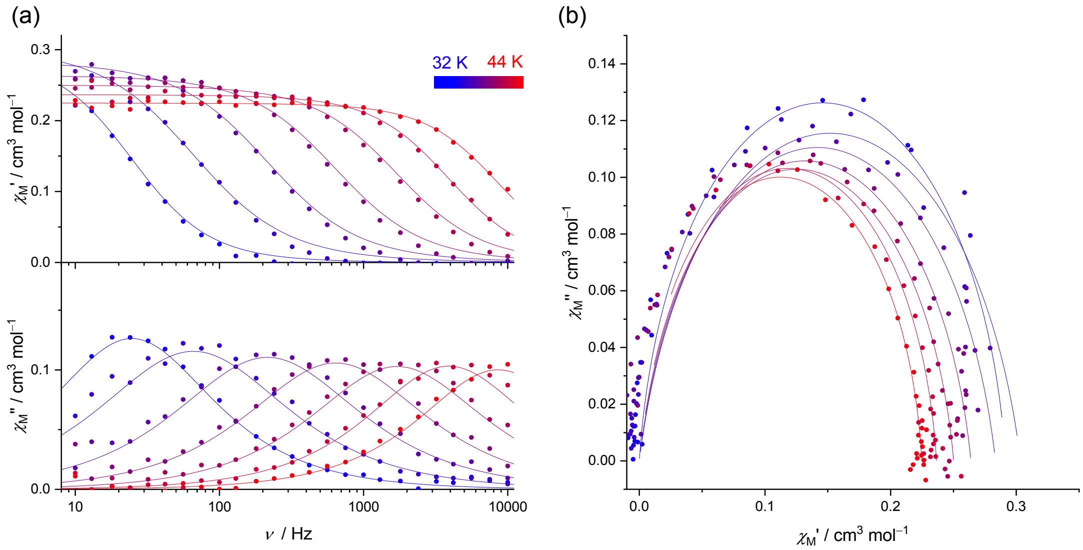

Figure S9. (a) AC magnetic susceptibilities and (b) Argand plots of $\mathbf{1}^{-*}$ at 2000 Oe bias dc field. Solid curves represent the fit using generalized Debye model equations.

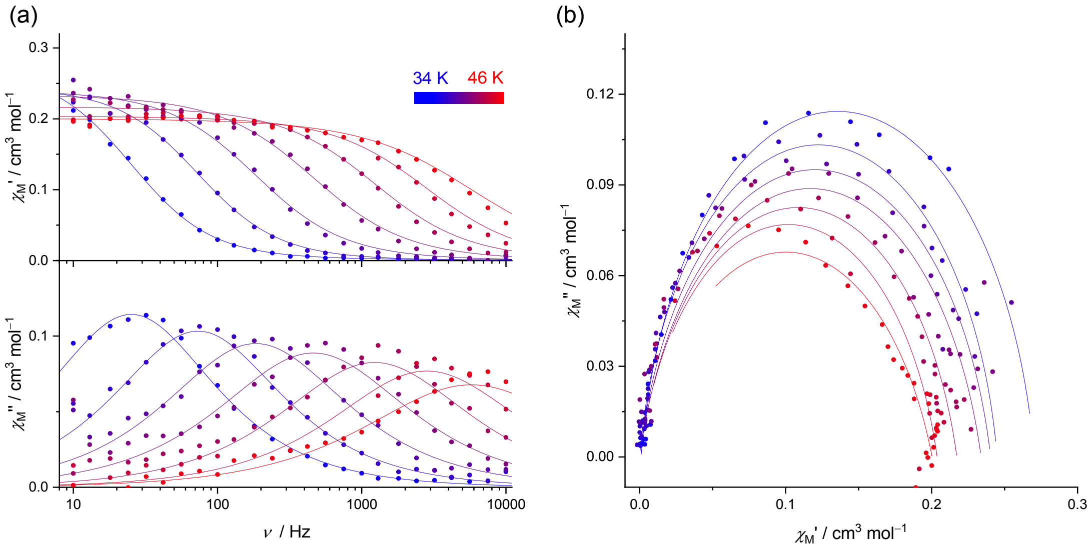

Figure S10. (a) AC magnetic susceptibilities and (b) Argand plots of **1**$^{+*}$ without a bias dc field. Solid curves represent the fit using generalized Debye model equations.

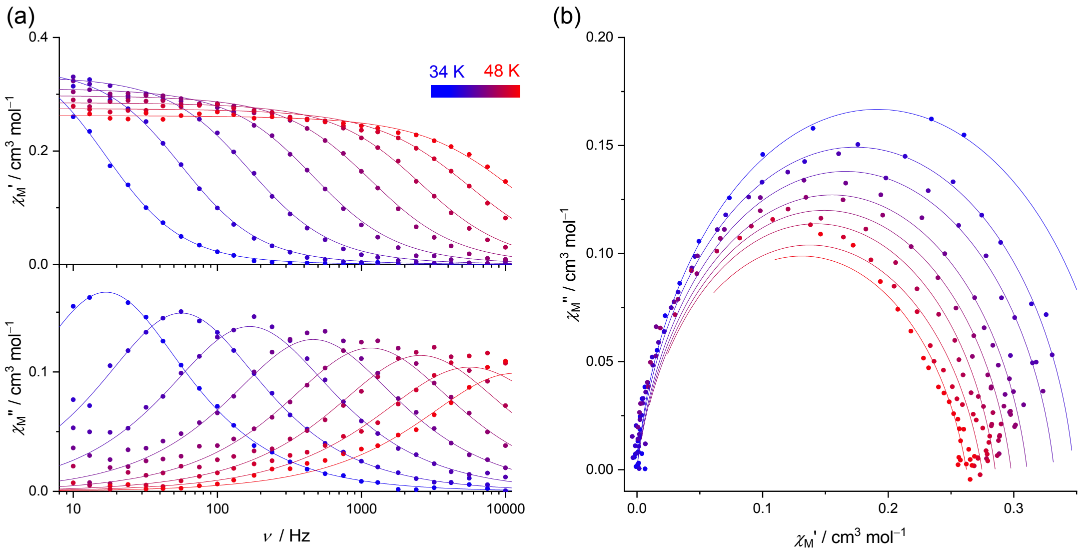

Figure S11. (a) AC magnetic susceptibilities and (b) Argand plots of **1**$^{+*}$ at 2000 Oe bias dc field. Solid curves represent the fit using generalized Debye model equations.

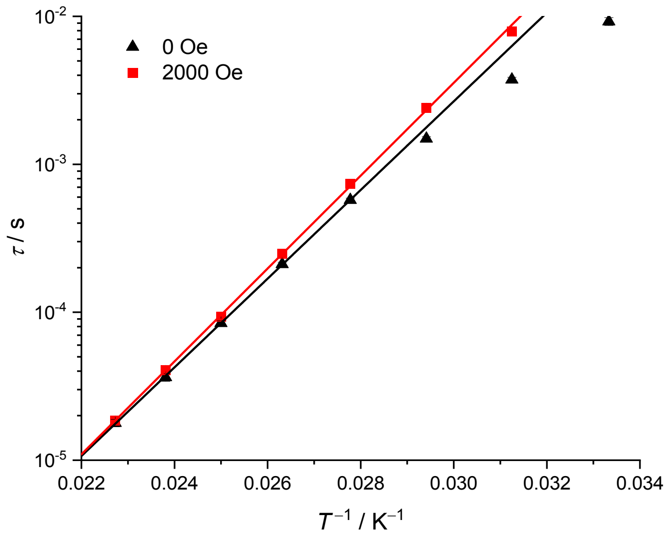

Figure S12. Arrhenius plots of $\mathbf{1}^{-*}$ with and without a dc bias field. Solid curves represent a fit using Eq. 1 from the main text. The optimized parameters are summarized in Table S3. Due to the linearity of the data, the Raman process was not considered in the fitting of this data. To exclude the small contribution of the Raman process, data points in the *T* range of 36-44 K were used for the Arrhenius fit.

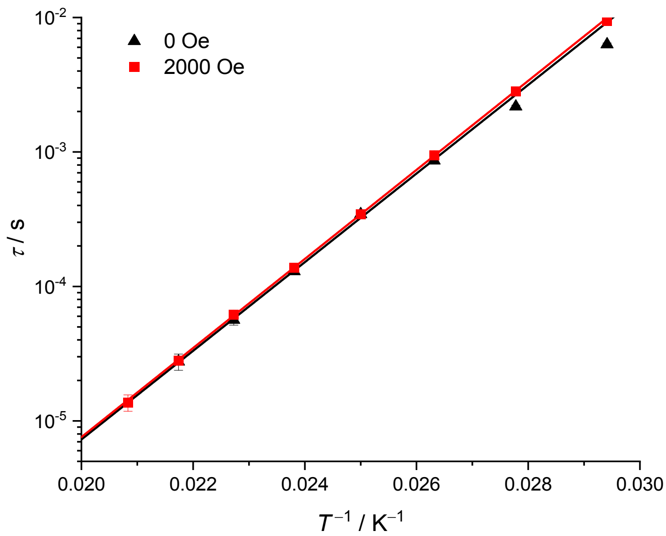

Figure S13. Arrhenius plots of $\mathbf{1}^{+*}$ with and without a dc bias field. Solid curves represent a fit using Eq. 1 from the main text. The optimized parameters are summarized in Table S3. Due to linearity of the data, the Raman process was not considered in the fitting of this data. To exclude the small contribution of the Raman process, data points in the *T* range of 40-46 K at 0 Oe and 42-48 K at 2000 Oe were used for the Arrhenius fit.

Table S3. Optimized parameters obtained by fitting the Arrhenius plots of $\mathbf{1}^{-*}$ and $\mathbf{1}^{+*}$.

	τ_0 / s	ΔE / cm^{-1}
$\mathbf{1}^{-*}$@0 Oe	$2.7(2) \times 10^{-12}$	480(2)
$\mathbf{1}^{-*}$@2000 Oe	$1.4(2) \times 10^{-12}$	502(4)
$\mathbf{1}^{+*}$@0 Oe	$1.9(6) \times 10^{-12}$	528(11)
$\mathbf{1}^{+*}$@2000 Oe	$1.8(5) \times 10^{-12}$	530(8)

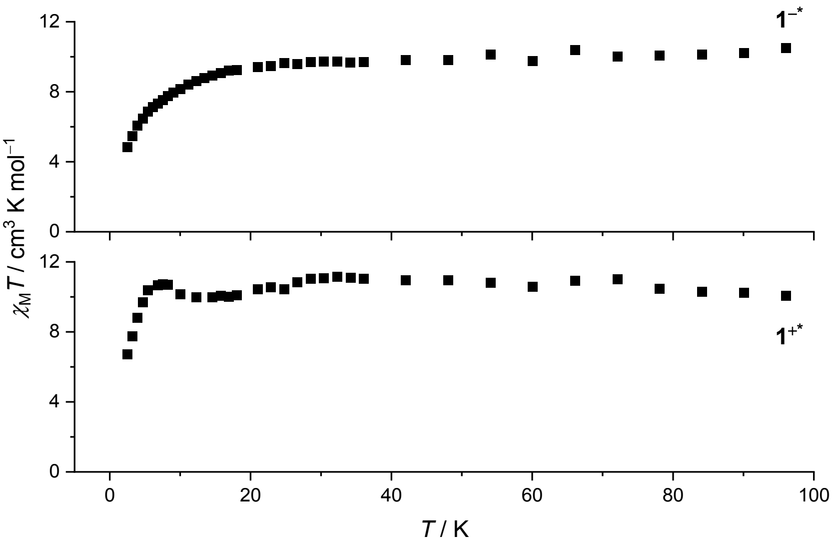

Figure S14. $\chi_M T$ vs T plots for $\mathbf{1}^{-*}$ and $\mathbf{1}^{+*}$ at 1000 Oe dc magnetic field.

Table S4. Optimized parameters obtained by fitting the ac magnetic susceptibilities of 1^{-} at 0 Oe.

T / K	χ_S / cm^3	dev(χ_S)	χ_T / cm^3	dev(χ_T)	τ / s	dev(τ / s)	α	dev(α)
10	0.0084	6.05E-04	1.12277	0.01268	0.2396	0.00558	0.26678	0.00342
12	0.00847	7.93E-04	0.88498	0.00856	0.13103	0.00253	0.23436	0.00424
13	0.00911	8.34E-04	0.80075	0.00687	0.10136	0.00171	0.21954	0.00438
15	0.00886	9.94E-04	0.67634	0.00531	0.06471	9.83E-04	0.19808	0.0051
18	0.00963	9.08E-04	0.54857	0.00304	0.03698	4.05E-04	0.17251	0.00469
20	0.00873	0.001	0.48996	0.00269	0.02699	3.06E-04	0.16499	0.00524
25	0.00944	8.52E-04	0.38625	0.00151	0.01355	1.25E-04	0.14404	0.00474
27	0.00895	9.40E-04	0.35772	0.00144	0.01019	1.02E-04	0.13599	0.00529
29	0.0089	9.52E-04	0.33153	0.00122	0.00718	7.08E-05	0.12159	0.00536
31	0.00949	8.55E-04	0.30803	8.81E-04	0.00443	3.70E-05	0.09785	0.00471
33	0.00819	8.50E-04	0.28892	6.57E-04	0.00229	1.72E-05	0.08563	0.00432
35	0.00734	6.75E-04	0.27175	3.59E-04	0.00103	5.36E-06	0.07439	0.00299
37	0.0088	0.00104	0.25618	3.37E-04	4.41E-04	3.00E-06	0.05979	0.00378
38	0.00768	0.00175	0.25021	4.07E-04	2.82E-04	3.05E-06	0.0569	0.00545
40	0	0.00272	0.23756	2.44E-04	1.16E-04	1.85E-06	0.04832	0.00528
43	0.02294	0.01262	0.22106	2.12E-04	4.15E-05	3.32E-06	0.00549	0.01262

Table S5. Optimized parameters obtained by fitting the ac magnetic susceptibilities of 1^{-} at 2000 Oe.

T / K	χ_S / cm^3	dev(χ_S)	χ_T / cm^3	dev(χ_T)	τ / s	dev(τ / s)	α	dev(α)
27	0.00427	4.66E-04	0.35587	0.00591	0.15784	0.00399	0.09127	0.00717
29	0.00463	4.30E-04	0.33167	0.00198	0.06166	5.92E-04	0.09393	0.00437
31	0.00328	5.63E-04	0.30935	0.00118	0.01967	1.52E-04	0.09726	0.00424
33	0.00608	8.36E-04	0.28894	9.83E-04	0.006	5.43E-05	0.0845	0.0052
35	0.00213	9.23E-04	0.27238	6.44E-04	0.00184	1.49E-05	0.08997	0.00461
38	0.00162	0.00196	0.25037	5.55E-04	3.69E-04	4.64E-06	0.07026	0.0066
40	0	0.00532	0.23778	5.74E-04	1.36E-04	4.37E-06	0.06539	0.01132
43	0	0.05052	0.22064	8.54E-04	4.19E-05	1.19E-05	0	0.04558

Table S6. Optimized parameters obtained by fitting the ac magnetic susceptibilities of 1+ at 0 Oe.

T / K	χ_S / cm^3	dev(χ_S)	χ_T / cm^3	dev(χ_T)	τ / s	dev(τ / s)	α	dev(α)
15	0.01446	0.00104	0.96148	0.01534	0.19388	0.00806	0.3797	0.0051
20	0.01786	0.00148	0.6429	0.00835	0.06589	0.00209	0.32191	0.00736
25	0.01994	0.00168	0.48481	0.00516	0.03099	7.85E-04	0.27453	0.00878
30	0.02152	0.00172	0.39007	0.0034	0.0166	3.63E-04	0.23169	0.00952
35	0.02285	0.00159	0.32434	0.00197	0.00762	1.34E-04	0.17496	0.00893
40	0.02213	0.0012	0.27741	7.06E-04	0.00176	1.78E-05	0.10877	0.00561
41	0.02264	0.0011	0.26998	5.31E-04	0.00122	1.05E-05	0.09611	0.0048
42	0.02368	0.00101	0.26406	3.92E-04	8.35E-04	6.18E-06	0.0846	0.00406
43	0.02358	0.00105	0.25719	3.11E-04	5.68E-04	4.08E-06	0.07637	0.00376
44	0.02479	0.00111	0.25084	2.43E-04	3.89E-04	2.85E-06	0.06631	0.00351
45	0.02336	0.0014	0.24449	2.10E-04	2.65E-04	2.41E-06	0.06042	0.00374
46	0.02385	0.0017	0.23867	1.65E-04	1.84E-04	2.03E-06	0.05094	0.00373
47	0.02125	0.00285	0.2334	1.62E-04	1.25E-04	2.32E-06	0.04608	0.00482

Table S7. Optimized parameters obtained by fitting the ac magnetic susceptibilities of 1+ at 2000 Oe.

T / K	χ_S / cm^3	dev(χ_S)	χ_T / cm^3	dev(χ_T)	τ / s	dev(τ / s)	α	dev(α)
35	0.00535	5.06E-04	0.37819	0.00164	0.04115	3.20E-04	0.12354	0.00373
36	0.00609	4.80E-04	0.36353	0.00111	2.55E-02	1.52E-04	0.10983	0.00318
37	0.00523	5.65E-04	0.35288	9.82E-04	1.55E-02	9.37E-05	0.10665	0.00336
38	0.00535	5.39E-04	0.34187	7.22E-04	9.32E-03	4.82E-05	0.09914	0.00293
39	0.00603	5.65E-04	0.3323	5.96E-04	5.63E-03	2.77E-05	0.09138	0.00283
40	0.00572	5.75E-04	0.32378	4.81E-04	3.41E-03	1.55E-05	0.08687	0.00263
41	0.00627	7.54E-04	0.31567	4.99E-04	2.09E-03	1.14E-05	0.08431	0.00314
42	0.0073	9.07E-04	0.30773	4.68E-04	1.29E-03	7.69E-06	0.07986	0.00342
43	0.00834	0.00125	0.30116	4.97E-04	8.29E-04	6.19E-06	0.0741	0.0042
44	0.00921	0.00148	0.29454	4.37E-04	5.34E-04	4.39E-06	0.06798	0.00437
45	0.01115	0.0015	0.28696	3.11E-04	3.49E-04	2.80E-06	0.06366	0.00381
46	0.01521	0.00178	0.28042	2.48E-04	2.35E-04	2.21E-06	0.04966	0.00384
47	0.0159	0.00303	0.27463	2.57E-04	1.58E-04	2.55E-06	0.04583	0.00518
48	0.02135	0.0043	0.26908	2.14E-04	1.10E-04	2.56E-06	0.03207	0.00587

Table S8. Optimized parameters obtained by fitting the ac magnetic susceptibilities of 1⁻* at 0 Oe.

T / K	χ_S / cm^3	dev(χ_S)	χ_T / cm^3	dev(χ_T)	τ / s	dev(τ / s)	α	dev(α)
30	0	0.00176	0.38804	0.0125	0.00923	5.64076E-4	0.20593	0.01741
32	0	0.00204	0.3308	0.00648	0.00373	1.39514E-4	0.16595	0.01647
34	0	0.00246	0.30215	0.00431	0.00149	4.7712E-5	0.1485	0.01655
36	0	0.00277	0.28078	0.00295	5.73392E-4	1.66409E-5	0.12527	0.01591
38	0	0.00366	0.2648	0.00236	2.11223E-4	6.80009E-6	0.13353	0.01723
40	0	0.0052	0.25116	0.00198	8.44629E-5	3.28765E-6	0.12726	0.0196
42	0	0.00889	0.2386	0.00178	3.63315E-5	2.16732E-6	0.10744	0.02533
44	0	0.00895	0.22672	8.47126E-4	1.78492E-5	1.03048E-6	0.07574	0.01835

Table S9. Optimized parameters obtained by fitting the ac magnetic susceptibilities of 1⁻* at 2000 Oe.

T / K	χ_S / cm^3	dev(χ_S)	χ_T / cm^3	dev(χ_T)	τ / s	dev(τ / s)	α	dev(α)
32	0	0.0024	0.32812	0.01395	0.00792	5.75418E-4	0.14581	0.02623
34	0	0.0029	0.3034	0.00688	0.00241	1.13381E-4	0.17128	0.02217
36	0	0.00308	0.28348	0.00374	7.38595E-4	2.61589E-5	0.15688	0.01846
38	0	0.0044	0.26393	0.00308	2.48302E-4	1.0085E-5	0.13968	0.02163
40	0	0.00439	0.25015	0.00178	9.32015E-5	3.12555E-6	0.12382	0.01724
42	0	0.00666	0.2365	0.00151	4.08147E-5	1.79486E-6	0.08668	0.02058
44	0	0.00925	0.22471	9.23725E-4	1.86004E-5	1.11572E-6	0.07359	0.01968

Table S10. Optimized parameters obtained by fitting the ac magnetic susceptibilities of 1[+*] at 0 Oe.

T / K	χ_S / cm^3	dev(χ_S)	χ_T / cm^3	dev(χ_T)	τ / s	dev(τ / s)	α	dev(α)
34	9.66048E-4	8.8555E-4	0.27032	0.00401	0.0063	1.51112E-4	0.10383	0.01062
36	0	0.00142	0.24488	0.00301	0.00217	5.25899E-5	0.10794	0.01312
38	0	0.00317	0.24045	0.00416	8.62872E-4	3.82395E-5	0.14829	0.02335
40	0	0.00498	0.23391	0.0041	3.44486E-4	1.99836E-5	0.17321	0.02949
42	0	0.0051	0.21729	0.00244	1.29665E-4	6.60055E-6	0.17288	0.02456
44	0	0.01014	0.20377	0.00265	5.63123E-5	4.83587E-6	0.17686	0.04338
46	0	0.01356	0.20036	0.00188	2.7598E-5	3.78815E-6	0.24261	0.03548

Table S11. Optimized parameters obtained by fitting the ac magnetic susceptibilities of 1[+*] at 2000 Oe.

T / K	χ_S / cm^3	dev(χ_S)	χ_T / cm^3	dev(χ_T)	τ / s	dev(τ / s)	α	dev(α)
34	0	6.55724E-4	0.38237	0.0044	0.00944	1.68744E-4	0.08686	0.00673
36	0	0.00121	0.34774	0.00299	0.00283	4.43361E-5	0.09686	0.00848
38	0	0.00239	0.33211	0.00326	9.4888E-4	2.26449E-5	0.11711	0.01318
40	0	0.00366	0.31055	0.00304	3.43896E-4	1.05578E-5	0.12647	0.01679
42	0	0.00445	0.29785	0.00238	1.37638E-4	4.33787E-6	0.13642	0.01661
44	0	0.00653	0.2852	0.00196	6.18543E-5	2.5702E-6	0.14248	0.01903
46	0	0.0119	0.27468	0.00175	2.81812E-5	2.18417E-6	0.175	0.02448
48	0	0.0208	0.26231	0.00142	1.36913E-5	1.90525E-6	0.17763	0.0297

Theoretical calculations

The restricted complete active-space self-consistent-field (CASSCF) method was used to get the detailed information about the ligand-field splitting of Tb^{3+} ions.[11] RASSCF and RASSI modules of the Molcas 8.2 software package[12] were used for RASSCF calculations and inclusion of the spin-orbit coupling (SOC), respectively. SINGLE_ANISO and POLY_ANISO modules were used for calculating the magnetic properties. Molecular geometries for the calculations were taken from the crystal structures. To reduce the computational costs, all the *n*-butoxy chains on the present samples were replaced with the methoxy groups. Eight electrons in the seven 4f-orbitals were selected as the active space ((8,7)-RASSCF). All the septet states (7), the quintet states (140) and the triplet states (588) were used to get the SOC states. The ANO-RCC-VDZP basis set was used for Tb and ANO-RCC-VDZ basis sets were used for all other atoms.[13-15]

Table S12. Energy level of the $^7F_6$ states of $\mathbf{1}^-$ and $\mathbf{1}^+$.

	$\mathbf{1}^-$	$\mathbf{1}^+$
State	E/cm^{-1}	E/cm^{-1}
1	0	0
2	0.000	0.000
3	324.600	321.866
4	324.614	321.878
5	536.150	523.950
6	536.219	524.475
7	632.432	612.245
8	642.995	620.577
9	663.931	637.940
10	699.409	659.940
11	701.240	663.181
12	742.017	681.632
13	742.190	682.376

Table S13. Wave function composition (in %) of the $^{7}F_{6}$ states of 1^{-}.

m_J	w.f. 1	w.f. 2	w.f. 3	w.f. 4	w.f. 5	w.f. 6	w.f. 7	w.f. 8	w.f. 9	w.f.	w.f.	w.f.	w.f.
-6	69.60	71.70	0.00	0.00	1.50	1.50	0.20	0.20	0.20	0.00	0.20	0.00	0.10
-5	0.00	0.00	70.50	70.60	1.10	1.10	4.00	4.40	1.10	2.30	0.20	1.00	0.40
-4	1.50	1.60	1.00	1.00	69.40	69.50	3.90	5.50	11.40	1.00	12.00	2.40	5.30
-3	0.10	0.10	4.70	4.60	3.60	3.60	58.70	66.70	11.00	38.60	4.60	17.70	9.70
-2	0.00	0.00	0.30	0.30	12.70	12.40	6.10	9.70	52.20	16.90	67.10	25.70	37.10
-1	0.00	0.00	0.40	0.30	0.90	0.50	38.50	19.70	5.50	56.40	17.90	53.00	42.30
0	0.00	0.00	0.20	0.00	3.70	3.40	4.20	5.50	63.00	8.70	5.00	49.30	58.50
1	0.00	0.00	0.40	0.30	0.90	0.50	38.50	19.70	5.50	56.40	17.90	53.00	42.30
2	0.00	0.00	0.30	0.30	12.70	12.40	6.10	9.70	52.20	16.90	67.10	25.70	37.10
3	0.10	0.10	4.70	4.60	3.60	3.60	58.70	66.70	11.00	38.60	4.60	17.70	9.70
4	1.60	1.50	1.00	1.00	69.40	69.50	3.90	5.50	11.40	1.00	12.00	2.40	5.30
5	0.00	0.00	70.50	70.50	1.10	1.10	4.00	4.40	1.10	2.30	0.20	1.00	0.40
6	71.70	69.60	0.00	0.00	1.50	1.50	0.20	0.20	0.20	0.00	0.20	0.00	0.10

Table S14. Wave function composition (in %) of the $^{7}F_{6}$ states of 1^{+}.

m_J	w.f. 1	w.f. 2	w.f. 3	w.f. 4	w.f. 5	w.f. 6	w.f. 7	w.f. 8	w.f. 9	w.f.	w.f.	w.f.	w.f.
-6	73.10	68.20	0.00	0.00	0.40	0.40	0.00	0.00	0.00	0.10	0.10	0.00	0.10
-5	0.00	0.00	70.70	70.70	0.60	0.60	1.60	1.60	0.40	0.40	0.40	0.10	0.10
-4	0.50	0.40	0.60	0.60	70.30	70.50	2.20	2.90	6.90	2.50	4.90	1.10	1.80
-3	0.00	0.00	1.60	1.60	2.50	2.60	63.60	69.50	8.50	29.50	3.90	8.40	8.60
-2	0.00	0.00	0.20	0.20	6.40	5.10	4.30	9.00	58.80	12.80	67.80	37.30	15.10
-1	0.10	0.10	0.40	0.20	1.90	0.80	30.20	8.00	1.90	62.10	19.00	11.10	68.30
0	0.00	0.00	0.50	0.00	4.80	0.40	4.80	5.30	53.30	13.70	0.80	82.70	7.60
1	0.10	0.10	0.40	0.20	1.90	0.80	30.20	8.00	1.90	62.10	19.00	11.10	68.30
2	0.00	0.00	0.20	0.20	6.40	5.10	4.30	9.00	58.80	12.80	67.80	37.30	15.10
3	0.00	0.00	1.60	1.60	2.50	2.60	63.60	69.50	8.50	29.50	3.90	8.40	8.60
4	0.40	0.50	0.60	0.60	70.30	70.50	2.20	2.90	6.90	2.50	4.90	1.10	1.80
5	0.00	0.00	70.70	70.70	0.60	0.60	1.60	1.60	0.40	0.40	0.40	0.10	0.10
6	68.20	73.10	0.00	0.00	0.40	0.40	0.00	0.00	0.00	0.10	0.10	0.00	0.10

Table S15. Main values of the *g*-tensor of the ground (G_0) and excited (Ex) quasi-Kramers doublets.

	1^-			1^+		
	g_x	g_y	g_z	g_x	g_y	g_z
G_0	0	1.0E-08	17.9	0	2.9E-08	17.9
Ex1	1E-09	1.3E-08	14.6	0	9.5E-08	14.6
Ex2	0	3.9E-08	11.4	0	7.2E-08	11.6
Ex3	3.0E-08	5.3E-08	7.74	2.0E-08	1.69E-07	8.13
Ex4	1.68E-07	3.87E-07	9.45	5.97E-07	1.98E-06	10.48
Ex5	1.02E-06	6.39E-06	6.06	1.20E-06	2.43E-06	3.66

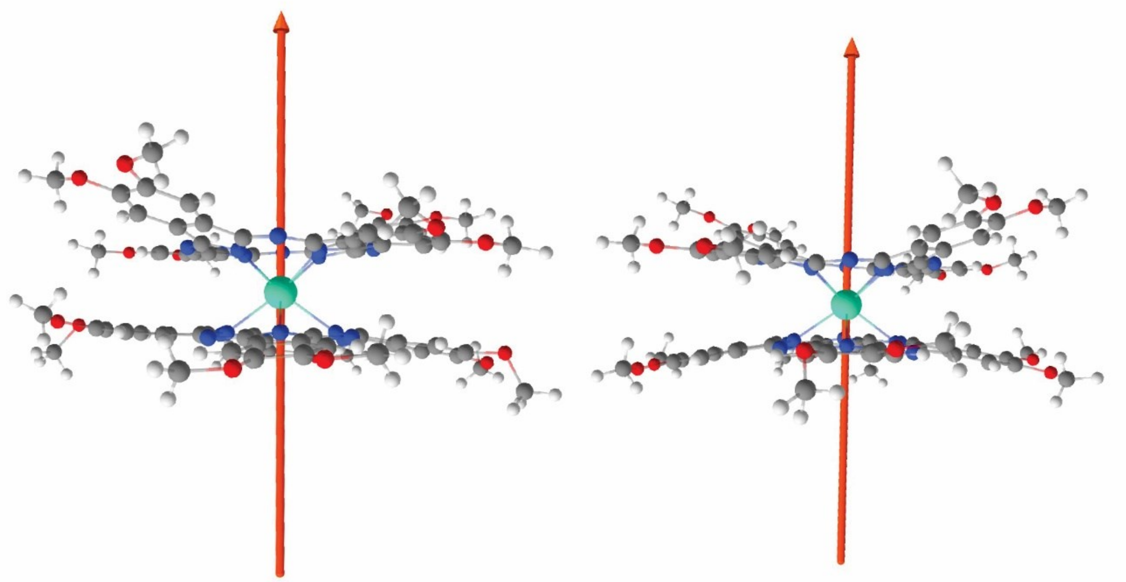

Figure S15. Calculated easy axis direction of **1**$^{-}$. The molecular fragment is shown from two perspectives, differing by ca. 90 degrees from one another with respect to the rotation around the axis perpendicular to two ligands.

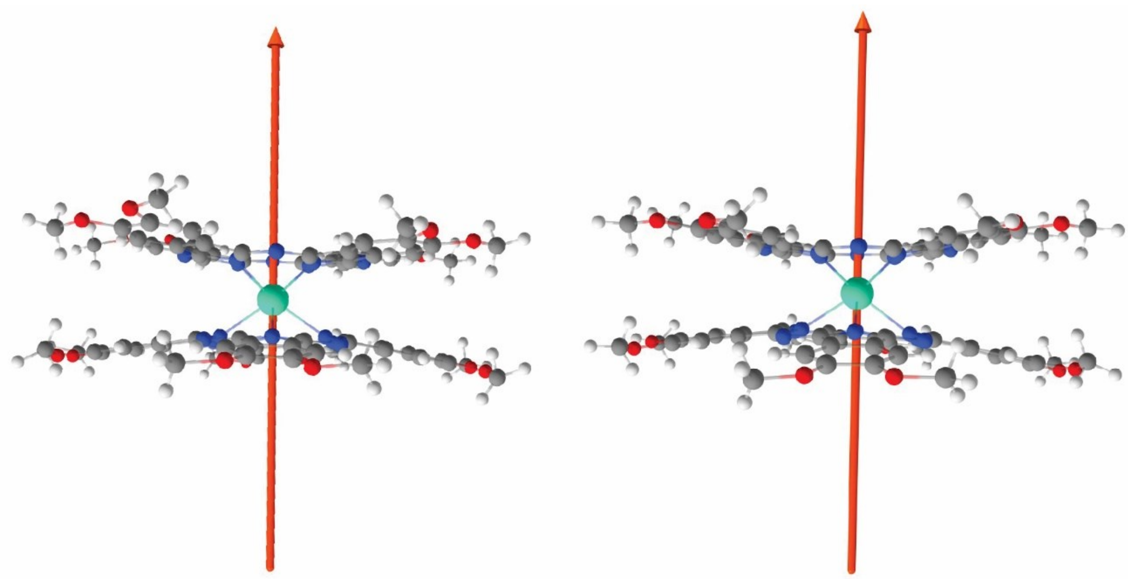

Figure S16. Calculated easy axis direction of **1**$^{+}$. The molecular fragment is shown from two perspectives, differing by ca. 90 degrees from one another with respect to the rotation around the axis perpendicular to two ligands.

References

[1] CrysAlisPRO, Oxford Diffraction /Agilent Technologies UK Ltd, Yarnton, England.

[2] G. Sheldrick, *Acta Crystallogr. A* **2008**, *64*, 112-122.

[3] Yadokari-XG, Software for Crystal Structure Analyses, K. Wakita (2001); Release of Software (Yadokari-XG 2009) for Crystal Structure Analyses, C. Kabuto, S. Akine, T. Nemoto, and E. Kwon, J. Cryst. Soc. Jpn., 51(3), 218-224 (2009).

[4] A. Spek, *Acta Crystallogr. C* **2015**, *71*, 9-18.

[5] C. F. Macrae, I. Sovago, S. J. Cottrell, P. T. A. Galek, P. McCabe, E. Pidcock, M. Platings, G. P. Shields, J. S. Stevens, M. Towler, P. A. Wood, *J. Appl. Crystallogr.* **2020**, *53*, 226-235.

[6] K. Katoh, Y. Horii, N. Yasuda, W. Wernsdorfer, K. Toriumi, B. K. Breedlove, M. Yamashita, *Dalton Trans.* **2012**, *41*, 13582.

[7] F. Weigend, R. Ahlrichs, *Phys. Chem. Chem. Phys.* **2005**, *7*, 3297-3305.

[8] D. Andrae, U. Häußermann, M. Dolg, H. Stoll, H. Preuß, *Theor. Chim. Acta* **1990**, *77*, 123-141.

[9] N. Frank, *Wiley. Interdiscip. Rev. Comput. Mol. Sci.* **2012**, *2*, 73-78.

[10] F. Weigend, *Phys. Chem. Chem. Phys.* **2006**, *8*, 1057–1065.

[11] L. Ungur, L. F. Chibotaru, *Phys. Chem. Chem. Phys.* **2011**, *13*, 20086-20090.

[12] F. Aquilante, J. Autschbach, R. K. Carlson, L. F. Chibotaru, M. G. Delcey, L. De Vico, I. Fdez. Galván, N. Ferré, L. M. Frutos, L. Gagliardi, M. Garavelli, A. Giussani, C. E. Hoyer, G. Li Manni, H. Lischka, D. Ma, P. Å. Malmqvist, T. Müller, A. Nenov, M. Olivucci, T. B. Pedersen, D. Peng, F. Plasser, B. Pritchard, M. Reiher, I. Rivalta, I. Schapiro, J. Segarra-Martí, M. Stenrup, D. G. Truhlar, L. Ungur, A. Valentini, S. Vancoillie, V. Veryazov, V. P. Vysotskiy, O. Weingart, F. Zapata, R. Lindh, *J. Comput. Chem.* **2016**, *37*, 506-541.

[13] B. O. Roos, R. Lindh, P.-Å. Malmqvist, V. Veryazov, P.-O. Widmark, *J. Phys. Chem. A* **2004**, *108*, 2851-2858.

[14] B. O. Roos, R. Lindh, P.-Å. Malmqvist, V. Veryazov, P.-O. Widmark, A. C. Borin, *J. Phys. Chem. A* **2008**, *112*, 11431-11435.

[15] P.-O. Widmark, P.-Å. Malmqvist, B. O. Roos, *Theor. Chim. Acta* **1990**, *77*, 291-306.